Earth Evolution Sciences, Vol. 14, pp. 3-8, March 1, 2020

In-situ EPMA dating of monazites in granulites from collisional orogens in southern India and southern Africa

Hikaru Kadowaki [a] and Toshiaki Tsunogae [b,c,*]

[a] *Graduate School of Life and Environmental Sciences, University of Tsukuba, Ibaraki 305-8572, Japan*
[b] *Faculty of Life and Environmental Sciences, University of Tsukuba, Ibaraki 305-8572, Japan*
[c] *Department of Geology, University of Johannesburg, Auckland Park 2006, South Africa*

** Corresponding author*

Abstract

The EPMA U-Th-Pb dating technique of monazite has been newly developed using a JEOL JXA-8530F microprobe at the Chemical Analysis Division of the Research Facility Center for Science and Technology, the University of Tsukuba. A natural cheralite from southern India was adopted for the standard material of Th, together with other oxide, phosphate, and metal standards. The application of the technique on a composite monazite grain in a metasediment from the Trivandrum Block, southern India, gave a metamorphic age of 544 ± 17 Ma, which is nearly consistent with the published near-peak metamorphic age of monazites (555.1 ± 8.1 Ma) from the same sample analyzed by LA-ICP-MS. Application of the analytical technique on monazites from the Limpopo Complex in southern Africa yielded a Paleoproterozoic metamorphic age (1923 ± 19 Ma), also consistent with published results. The dating technique can be thus applicable to various high-grade metamorphic rocks for unraveling thermal history of orogenic belts.

Keywords: monazite geochronology, CHIME, Trivandrum Block, Limpopo Complex

Introduction

Monazite often contains significant quantity of thorium and uranium, while the amount of initial Pb is little compared to radiogenic Pb (Williams et al., 1983; Corfu, 1988; Suzuki and Kato, 2008). Therefore, EPMA (electron microprobe) U-Th-Pb dating (or CHIME dating; Suzuki and Adachi, 1991a, 1991b, 1994) of monazite has attracted many geologists because of its advantages of quickness and relatively high reliability (Montel et al., 1996; Williams et al., 2006; Cocherie and Albarede, 2001). Particularly, the technique allows us to perform *in-situ* analysis of complex monazite grains in thin sections with high spatial resolution. The dating technique has been therefore widely applied to various metamorphic rocks for unraveling texture-based thermal history of orogenic belts (e.g., Santosh et al., 2003). In this study, we newly developed *in-situ* EPMA dating technique of monazite using a JEOL JXA-8530F microprobe installed at the Chemical Analysis Division of the Research Facility Center for Science and Technology, the University of Tsukuba. The age results are compared with those in published papers for the evaluation of the technique.

Analytical procedure

The monazite dating was carried out using JEOL JXA-8530F microprobe under an accelerating voltage of 20 kV, beam currents of 100 nA for monazites and 10 nA for standard materials, and a beam diameter of 5 micron. The data were regressed using an oxide-ZAF correction program supplied by JEOL.

The standard materials adopted for quantitative analysis of monazite are galena (PbS) for Pb, metal uranium for U, natural cheralite for Th, end-member synthetic phosphates (XPO_4) for rare-earth elements (La, Ce, Pr, Nd, and Sm) and Y, $CePO_4$ for P, and wollastonite for Ca and Si. The composition of natural cheralite from southern India, which was adopted as our standard, was analyzed at JEOL laboratory at Akishima (Tokyo) on 16th of December 2019 using JEOL JXA-8230 microprobe. The cheralite composition is shown in Table 1. Peak and background counting times and the X-ray lines adopted in this study are summarized in Table 2. The X-ray lines used are U*M*β, Pb*M*α, Th*M*α, P*K*α, Si*K*α, Ca*K*α, Nd*L*β, Sm*L*α, Ce*L*α, La*L*α, Pr*L*β, and Y*L*α. They were carefully evaluated to avoid interferences. The counting time (peak + background) was 200 + 100 for U and Pb, 60 + 30 for Th, and 20 + 10 for each of the other elements.

The procedure of CHIME age calculation is summa-

Table 1. Composition of cheralite adopted as the standard material for thorium.

	average		error
SiO_2	5.02	±	0.10
CaO	1.40	±	0.01
ThO_2	26.96	±	0.28
UO_2	0.61	±	0.01
P_2O_5	22.72	±	0.17
Ce_2O_3	19.96	±	0.21
La_2O_3	7.78	±	0.09
Pr_2O_3	2.69	±	0.04
Nd_2O_3	11.88	±	0.09
Sm_2O_3	1.29	±	0.03
Total	100.31		

rized in Suzuki and Adachi (1991a, 1991b, 1994). For the calculation, we employed the software developed by Kato et al. (1999) with York (1966) method and decay constants from Steiger and Jäger (1977). The concentrations (in wt.%) of ThO_2, UO_2, and PbO obtained by EPMA analysis as well as relative analytical errors (in %) of the oxides were adopted. The relative analytical errors (E in %) of the EPMA analysis are determined by calculation using upper- and lower-background intensities ($BG+$ and $BG-$, respectively, in cps/μA), net intensities (Net in cps/μA), current value (C in nA), and measurement times (τ in second) for Th, U, and Pb as follow;

$$\frac{(BG+)+(BG-)}{2}\times C = I_{(background)} \quad (1)$$

$$\frac{(Net)\times C}{1000} = I_{(peak)} \quad (2)$$

$$I_{(peak)} + I_{(background)} = I \quad (3)$$

$$E(\%) = \frac{\sqrt{\left(I + I_{(background)}\right)\times\tau}}{\left(I - I_{(background)}\right)\times\tau}\times 100 \quad (4)$$

where I is intensity in cps. The E values are used for age calculations based on least squares method of York (1966).

Below, we briefly summarize the procedure of CHIME dating method based on Suzuki and Adachi (1991a, 1991b, 1994). In the first step, an apparent age 't' of each spot is determined by the following calculation;

$$\frac{PbO}{W_{Pb}} = \frac{ThO_2}{W_{Th}}\left\{exp\left(\lambda_{232}t-1\right)\right\} + \frac{UO_2}{W_U}\left\{\frac{exp\left(\lambda_{235}t\right)+137.88exp\left(\lambda_{238}t\right)}{138.88}-1\right\} \quad (5)$$

where W_{Pb} is molecular weight of Pb, and W_{Th} and W_U are molecular weight of Th (= 264) and U (= 270), respectively. W_{Pb} = 224 is adapted for ThO_2-rich minerals (e.g., monazite), whereas W_{Pb} = 222 is adapted for UO_2-rich minerals (e.g., zircon). In this equation, PbO, ThO_2, and UO_2 are concentration of PbO, ThO_2, and UO_2 (wt.%), respectively. λ_{232} (= 4.9475×10^{-11}/year), λ_{235} (= 9.8485×10^{-10}/year), and λ_{238} (= 1.55125×10^{-10}/year) are decay constants which are mentioned in Steiger and Jäger (1977). Current isotopic ratio of U ($^{238}U/^{235}U$ = 137.88; Steiger and Jäger, 1977) is used in this equation.

Using the apparent age (t), apparent amount of total ThO_2 (ThO_2*) and UO_2 (UO_2*) are computed for ThO_2-rich and UO_2-rich minerals as follow;

Table 2. List of analytical conditions of monazite.

Element	Channel	Crystal	X-ray line	Peak position (nm)	Background (+)	Background (-)	Peak counting time	Background counting time
Si	2	TAP	*K*α	77.285	5	5	20	10
Ca	4	PETH	*K*α	107.061	5	5	20	10
U	4	PETH	*M*α	118.49	0.7	0.5	200	100
Th	4	PETH	*M*α	132.018	5	4	60	30
Pb	1	PETH	*M*α	169.269	5	4	200	100
P	2	TAP	*K*α	66.679	5	5	10	5
La	1	LIFH	*L*α	185.313	5	5	20	10
Ce	1	LIFH	*L*α	178.975	5	5	20	10
Pr	1	LIFH	*L*β	157.023	2	2	20	10
Nd	1	LIFH	*L*β	150.65	1.2	5	20	10
Sm	1	LIFH	*L*β	138.893	1	1	20	10
Y	4	PETH	*L*α	206.241	5	5	20	10

$$ThO_2^* = ThO_2 + \frac{UO_2 \cdot W_{Th}}{W_U\left\{exp\left(\lambda_{232}t\right)-1\right\}} \cdot \left\{\frac{exp\left(\lambda_{232}t\right)+137.88exp\left(\lambda_{238}t\right)}{138.88}-1\right\} \quad (6)$$

(for ThO_2-rich mineral)

$$UO_2^* = UO_2 + \frac{138.88ThO_2 \cdot W_U\left\{exp\left(\lambda_{232}t\right)-1\right\}}{W_{Th}\left\{exp\left(\lambda_{235}t\right)+137.88exp\left(\lambda_{238}t\right)-138.88\right\}} \quad (7)$$

(for UO_2-rich mineral)

If all the portions in a single mineral grain is monogenetic, contain the same amount of initial Pb but different amounts of Th and U, and have remained in a closed system, all the analytical data will lie on a straight line (isochron) with a slope (m) and an intercept (b) in a ThO_2* or UO_2* versus PbO plot;

$$PbO = m \cdot ThO_2^* + b \quad (8)$$

(for ThO_2-rich mineral)

$$PbO = m \cdot UO_2^* + b \quad (9)$$

(for UO_2-rich mineral)

The best-fit regression line is calculated based on the procedure of York (1966), taking account of uncertainties (E) in the microprobe analyses. Then, the first approximate value of age (T) from the slope (m) of equations will be calculated by the following equations;

$$T = \frac{1}{\lambda_{232}} In\left(1 + m\frac{W_{Th}}{W_{Pb}}\right) \quad (10)$$

(for ThO_2-rich mineral)

$$m\frac{W_U}{W_{Pb}} = \frac{exp\left(\lambda_{235}T\right)+137.88exp\left(\lambda_{238}T\right)}{138.88}-1 \quad (11)$$

(for UO_2-rich mineral)

The intercept (b) of the regression line is inferred to represent the concentration (in wt.%) of the initial PbO. Recalculation of ThO_2* or UO_2* with estimated T instead of t provides reliable estimate of age and initial PbO.

Results and discussion

Khondalite from the Trivandrum Block

The Southern Granulite Terrane in India is composed of several Mesoarchean to Neoproterozoic granulite blocks intersected by Neoproterozoic to Cambrian suture/shear zones (e.g., Drury et al., 1984). The Trivandrum Block in the southern part of the terrane is composed dominantly of metasediments (khondalite and leptynite) and charnockite (Geological Survey of India, 1995a, 1995b). The block underwent high- to ultrahigh-temperature metamorphism (e.g., Chacko et al., 1987; Cenki et al., 2004; Morimoto et al, 2004; Tadokoro et al., 2008) during Neoproterozoic (e.g., Santosh et al., 2005, 2006). Kadowaki et al. (2019) obtained LA-ICP-MS monazite age of an ultrahigh-temperature (920–1030°C and 6.0–7.6 kbar) khondalite from the block, and reported a broad age range of 612 ± 11 Ma to 461 ± 7 Ma with two age peaks at 555.1 ± 8.1 Ma and 501.9 ± 8.5 Ma. Their U-Pb analysis was done using LA-ICP-MS instrument at the University of Adelaide. In this study, we adopted the same khondalite (sample KP5H) examined by Kadowaki et al. (2019) to compare the results of CHIME and LA-ICP-MS dating methods and evaluated the reliability of age results obtained in this study.

A thin section was used for the *in-situ* dating. The monazite examined in this study occurs as rounded to partly irregular mineral included in coarse-grained cordierite. A back-scattered electron (BSE) image of the monazite grain is shown in Figure 1a together with the positions of analyzed spots and ages. The grain is compositionally heterogeneous with thorium-rich (ThO_2 = 26.9 wt.%, bright BSE) and thorium-poor (ThO_2 = 7.5 wt.%, dark BSE) portions. The analyzed spot ages vary from 559 Ma to 517 Ma. The ages obtained from the Th-rich portion (537-531 Ma) are nearly consistent with the Th-poor portion (559-534 Ma). Figure 2a shows a ThO_2*-PbO plot with a calculated age and error in one sigma for all the analyzed nine spots. All the data are plotted on an isochron showing the age of 541 ± 17 Ma, which is nearly consistent with the older age peak (555.1 ± 8.1 Ma) of Kadowaki et al. (2019). As the analyzed monazite occurs as an inclusion in cordierite rather than in the matrix, the grain was probably not affected by the later ca. 502 Ma thermal event.

Pelitic granulite from the Limpopo Complex

The Limpopo Complex has been regarded as a classic example of collisional orogens formed by amalgamation of the Kaapvaal and Zimbabwe Cratons during Neoproterozoic (e.g., Roering et al., 1992), although some recent studies pointed out multiple collisional events during Neoarchean to Paleoproterozoic (e.g., Kröner et al., 2018). Particularly, the Central Zone of the Limpopo Complex is different from other portions of the complex because the zone underwent regional thermal event during Paleoproterozoic (ca. 2.0 Ga; Jaeckel et al.,1997). For example, Buick et al. (2006) obtained SHRIMP weighted mean

^{207}Pb-^{206}Pb monazite age of 2028 ± 3 Ma from garnet–cordierite–orthoamphibole gneisses from the western Central Zone, South Africa. Chudy et al. (2008) also obtained similar monazite age of 2015 ± 8 Ma from pelitic rocks of the Krone Metamorphic terrane, South Africa, by LA-ICP-MS. They regarded the age as the timing of Paleoproterozoic metamorphic overprint under amphibolite-facies condition. Slightly younger monazite age of 2002 ± 10 Ma was obtained for monazites from partially melted Fe-rich metagreywacke from Lose quarry in Botswana as the timing of incongruent biotite melting related to high-grade metamorphism (Chavagnac et al., 2001).

Samples C54D and C25A were collected from the Zimbabwean side of the Central Zone. The dominant lithologies of the area are pelitic gneiss, quartzite, mafic granulite, banded iron-formation, granitoid gneiss, and calc-silicate, which occur as banded gneisses with abundant N-S-trending foliation (e.g., van Biljon and Legg, 1983). Sample C54D is a garnet-bearing leucocratic rock comprising coarse-grained plagioclase, quartz, K-feldspar, garnet, and biotite. Its field occurrence as a leucocratic layer in pelitic gneiss suggest partial-melting origin of the rock. Sample C25A is a typical pelitic granulite that consists of garnet, biotite, quartz, plagioclase, K-feldspar, cordierite, and sillimanite, with accessory spinel, ilmenite, zircon, and monazite. Foliation of the rock is well defined by elongated biotite flakes. In this study we analyzed one representative monazite grain from each sample.

The analyzed monazite from sample C54D is subhedral and medium grained (~100 micron), and occurs as an inclusion in coarse-grained plagioclase. A BSE image of the monazite grain is shown in Figure 1b together with the positions of analyzed spots and ages. Similar to the monazite from southern India, the grain is chemically heterogeneous with Th-rich portions (bright BSE) and Th-poor (dark BSE) portions, although the variation of Th content is less (ThO_2 = 21.2 to 24.8 wt.%) than sample KP5H from southern India. The analyzed spot ages vary from 2021 Ma to 1787 Ma, but mostly 2010-1970 Ma. In contrast, the analyzed monazite from sample C25A, occurring as an inclusion in rim of garnet, is compositionally nearly homogeneous with no obvious heterogeneity in BSE image (Figure 1c). Its ThO_2 content shows a narrow range of 4.1 to 5.6 wt.%. The analyzed spot ages vary from 2108 Ma to 1981 Ma with an average age of 2052 Ma.

Figure 2b shows a ThO_2*-PbO plot with a calculated age and error in one sigma for all the analyzed spots from the two samples. All the data are plotted along an isochron showing the age of 1928 ± 19 Ma. The age is slightly younger than the obtained monazite ages (2020-2003 Ma) from the Central Zone, although similar ca. 1.9 Ga age of 1982 ± 38 Ma has been obtained based on garnet Sm-Nd age of garnet-bearing leucosome from Lose quarry (Botswana) as the timing of high-grade metamorphism (Chavagnac et al., 2001). It has to be noted that previous ages have been reported from South African and Botswanan side of the Central Zone, while this is the first report of monazite age from the Zimbabwean side. Therefore, the timing of high-grade metamorphism in the Zimbabwean side might be slightly younger.

Conclusion

The EPMA U-Th-Pb dating technique of monazite has been developed using a JEOL JXA-8530F microprobe at the Chemical Analysis Division of the Research Facility Center for Science and Technology. We applied the method to monazites from the Trivandrum Block (southern

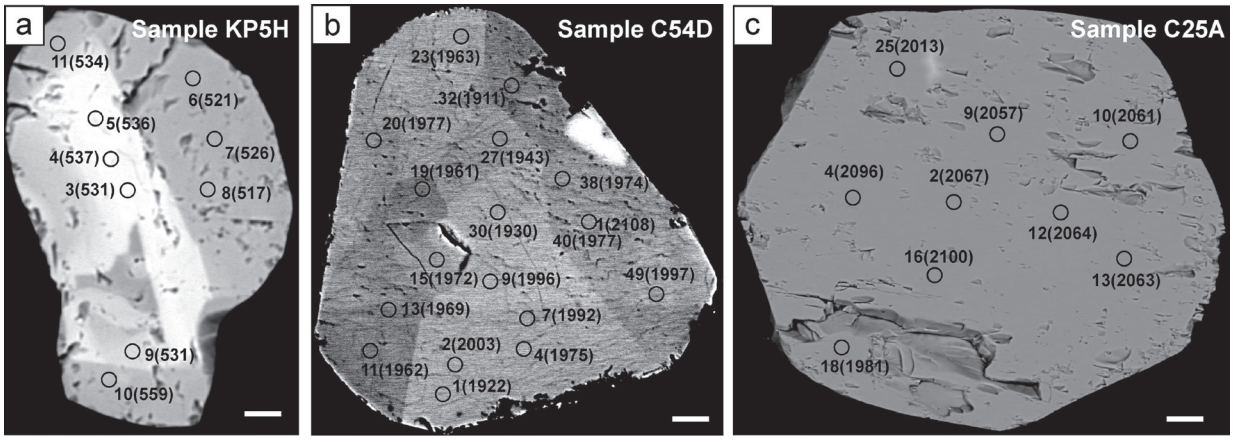

Fig. 1. Back-scattered electron images of monazites discussed in this study. (a) Monazite in sample KP5H from the Trivandrum Block. (b) Monazite in sample C54D from the Limpopo Complex. (c) Monazite in sample C25A from the Limpopo Complex. Circles indicate analytical points. Scale bars indicate 10 microns. Numbers indicate analytical numbers with ages in Ma (in parenthesis).

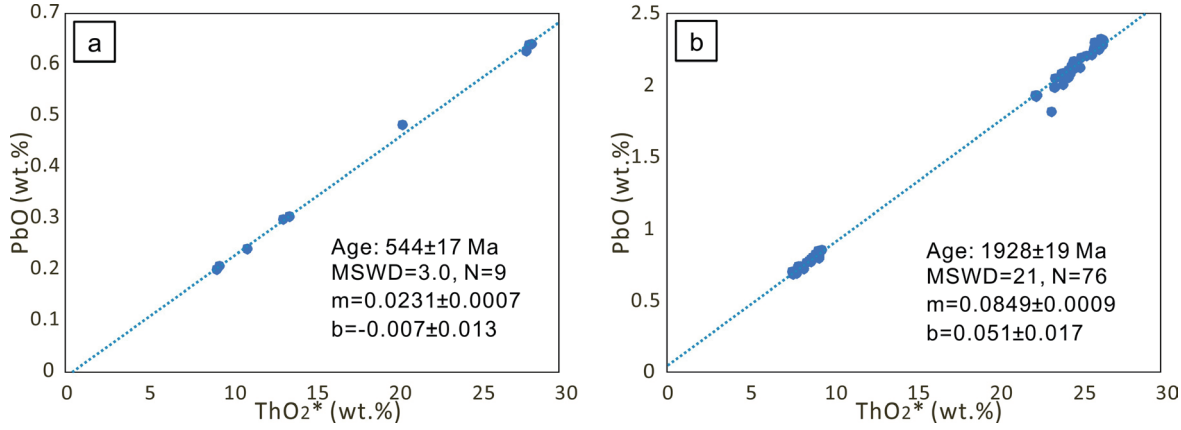

Fig. 2. ThO_2* versus PbO diagrams showing monazite compositions with regression lines for metasediment samples from the Trivandrum Block (a) and the Limpopo Complex (b).

India) and the Limpopo Complex (Zimbabwe), and obtained isochron ages of 541 ± 17 Ma and 1928 ± 19 Ma, respectively, which are nearly consistent with available ages from the regions. The results of this study confirmed that the dating technique can be applicable to Paleoproterozoic to Neoproterozoic high-grade metamorphic rocks for unraveling texture-based thermal history of orogenic belts.

Acknowledgement

Partial funding for this project was produced by a Grant-in-Aid for Scientific Research (B) from Japan Society for the Promotion of Science (JSPS) (No. 18H01300 and No. 19H19020) to Tsunogae. We thank Prof. Y. Arakawa and Mr. Y. Takamura for their constructive review comments. Mr. Y. Takamura is also acknowledged for his support on the standard analysis.

References

Buick, I.S., Hermann, J., Williams, I.S., Gibson, R.L., and Rubatto, D. (2006) A SHRIMP U–Pb and LA-ICP-MS trace element study of the petrogenesis of garnet–cordierite–orthoamphibole gneisses from the Central Zone of the Limpopo Belt, South Africa. *Lithos*, **88**, 150–172.

Cenki, B., Braun, I., and Bröcker, M. (2004). Evolution of the continental crust in the Kerala Khondalite Belt, southernmost India: evidence from Nd isotope mapping, U–Pb and Rb–Sr geochronology. *Precambrian Research, 134,* 275–292.

Chudy, T.C., Zeh, A., Gerdes, A., Klemd, R., and Barton, J.M., Jr. (2008) Palaeoarchaean (3.3 Ga) mafic magmatism and Palaeoproterozoic (2.02 Ga) amphibolite-facies metamorphism in the Central Zone of the Limpopo Belt: New geochronological, petrological and geochemical constraints from metabasic and metapelitic rocks from the Venetia area. *South African Journal of Geology*, **111**, 387–408.

Chavagnac, V., Kramers, J.D., Nägler, T.F., and Holzer, L. (2001) The behaviour of Nd and Pb isotopes during 2.0 Ga migmatization in paragneisses of the Central Zone of the Limpopo Belt (South Africa and Botswana). *Precambrian Research*, **112**, 51–86.

Chacko, T., Ravindra Kumar, G.R., and Newton, R.C. (1987) Metamorphic *P–T* conditions of the Kerala (South India) Khondalite Belt, a granulite facies supracrustal terrain. *Journal of Geology*, **95**, 343–358.

Cocherie, A. and Albarede, F. (2001) An improved U-Th-Pb age calculation for electronic microprobe dating of monazite: *Geochimica et Cosmochimica Acta*, **65**, 4509–4522.

Corfu, F. (1988) Differential response of U–Pb systems in coexisting accessory minerals, Winnipeg River Subprovince, Canadian Shield: implications for Archean crustal growth and stabilization. *Contributions to Mineralogy and Petrology*, **98**, 312–325.

Drury, S.A., Harris, N.B.W., Holt, R.W., Reeves-Smith, G.J., and Wightman, R.T. (1984) Precambrian tectonics and crustal evolution in South India. *The Journal of Geology*, **92**, 3–20.

Geological Survey of India (1995a). Geological and Mineral Map of Kerala.

Geological Survey of India (1995b). Geological and Mineral Map of Tamil Nadu and Pondichery.

Jaeckel, P., Kröner, A., Kamo, S.L., Brandl, G., and Wendt, J.I. (1997) Late Archaean to early Proterozoic granitoid magmatism and high-grade metamorphism in the central Limpopo belt, South Africa. *Journal of the Geological Society*, **154**, 25-44.

Kadowaki, H., Tsunogae, T., He, X.F., Santosh, M., Taka-

mura, Y., Shaji, E., and Tsutsumi, Y. (2019) Pressure-temperature-time evolution of ultrahigh-temperature granulites from the Trivandrum Block, southern India: implications for long-lived high-grade metamorphism. *Geological Journal*, **54**, 3041–3059.

Kato, T., Suzuki, K., and Adachi, M. (1999) Computer program for the CHIME age calculation. *The Journal of Earth and Planetary Sciences, Nagoya University*, **46**, 49–56

Kröner, A., Brandl, G., Brandt, S., Klemd, R., and Xie, H. (2018) Geochronological evidence for Archaean and Palaeoproterozoic polymetamorphism in the Central Zone of the Limpopo Belt, South Africa. *Precambrian Research*, **310**, 320–347.

Montel, J. M., Foret, S., Veschambre, M., Nicollet, C., and Provost, A. (1996) Electronic dating of monazite. *Chemical Geology*, **131**, 37–53.

Morimoto, T., Santosh, M., Tsunogae, T., and Yoshimura, Y. (2004) Spinel + quartz association from the Kerala Khondalites, southern India: evidence for ultra-high temperature metamorphism. *Journal of Mineralogical and Petrological Sciences*, **99**, 257–278.

Roering, C., van Reenen, D.D., de Wit, M.J., Smit, C.A., de Beer, J.H., and van Schalkwyk, J.F. (1992) Structural geological and metamorphic significance of the Kaapvaal Craton–Limpopo Belt contact. *Precambrian Research*, **55**, 69–80.

Santosh, M., Yokoyama, Y., Biju-Sekhar, S., and Rogers, J.J.W. (2003) Multiple tectonothermal events in the granulite blocks of southern India revealed from EPMA dating: implications on the history of supercontinents. *Gondwana Research*, **6**, 29–63.

Santosh, M., Collins, A. S., Morimoto, T., and Yokoyama, K. (2005). Depositional constraints and age of metamorphism in southern India: U–Pb chemical (EPMA) and isotopic (SIMS) ages from the Trivandrum Block. *Geological Magazine*, **142**, 1–14.

Santosh, M., Morimoto, T., and Tsutsumi, Y. (2006) Geochronology of the khondalite belt of Trivandrum Block, southern India: electron probe ages and implications for Gondwana tectonics. *Gondwana Research*, **9**, 261–278.

Steiger, R.H. and Jäger, E. (1977) Subcommission on geochronology: convention on the use of decay constants in geo- and cosmochronology. *Earth and Planetary Science Letters,* **36**, 359–362.

Suzuki, K. and Adachi, M. (1991a) Precambrian provenance and Silurian metamorphism of the Tsubonosawa paragneiss in the South Kitakami terrane, Northeast Japan. *Geochemical Journal*, **25**, 357–376.

Suzuki, K. and Adachi, M. (1991b) The chemical Th–U–total Pb isochron ages of zircon and monazite from the Gray Granite of the Hida terrane, Japan. *The Journal of Earth and Planetary Sciences, Nagoya University*, **38**, 11–37.

Suzuki, K. and Adachi, M. (1994) Middle Precambrian detrital monazite and zircon from the Hida gneiss on Oki-Dogo Island, Japan: their origin and implication for the correlation of the basement of Southwest Japan and Korea. *Tectonophysics*, **235**, 277-292.

Suzuki, K. and Kato, T. (2008) CHIME dating of monazite, xenotime, zircon and polycrase: Protocol, pitfalls and chemical criterion of possibly discordant age data. Gondwana Research, 14, 569–586.

Tadokoro, H., Tsunogae, T., and Santosh, M. (2008) Metamorphic *P–T* path of eastern Trivandrum Granulite Block, southern India: implications for regional correlation of lower crustal fragments. *Journal of Mineralogical and Petrological Sciences*, **103**, 279–284.

van Biljon, W.J. and Legg, J.H. (1983) The Limpopo Belt. *Special Publications of the Geological Society of South Africa*, **8**, 203pp.

Williams, I.S., Compston, W., and Chappell, B.W. (1983) Zircon and monazite U–Pb systems and histories of I-type magmas, Berridale Batholith, Australia. *Journal of Petrology*, **24**, 76–79.

Williams, M. L., Jercinovic, M. J., Goncalves, P., and Mahan, K. (2006) Format and philosophy for collecting, compiling, and reporting microprobe monazite ages. *Chemical Geology*, **225**, 1–15.

York, D. (1966) Least-squares fitting of a straight line. *Canadian Journal of Physics*, **44**, 1079–1088.